Kinetics of Melittin Self-Association in Aqueous Solution†

Gerhard Schwarz* and Georgi Beschiaschvili

Department of Biophysical Chemistry, Biocenter of the University of Basel, CH-4056 Basel, Switzerland

Received February 29, 1988; Revised Manuscript Received May 23, 1988

ABSTRACT: We have investigated the monomer–tetramer conversion of melittin in aqueous sodium sulfate solution at slightly alkaline pH by means of fluorescence. In a first series of experiments the degree of association at equilibrium was determined as a function of peptide concentration for various fixed salt concentrations. Then two types of kinetic measurements were carried out in a stopped-flow apparatus, setting the conditions so that either (i) the dissociation can be neglected (association kinetics approach) or (ii) fairly small perturbations of the equilibrium are induced (relaxation kinetics approach). The results reveal a second-order rate law for the forward (i.e., association) reaction and an order of one-half apparently applying to the dissociation process. The rate constant for the association increases with the salt concentration, and the one for dissociation decreases. The data can be quantitatively interpreted in terms of a simple mechanism. This comprises a comparatively slow dimerization involving the inherent change of secondary structure, followed by a practically diffusion-controlled dimer–dimer assembly. The intermediate dimer content amounts to about 1%.

The cationic peptide melittin is the main constituent of bee venom (Habermann, 1972). It can penetrate a lipid bilayer but nevertheless also dissolves well in an aqueous solvent (Knöppel et al., 1979). This peculiarity has given rise to a wide range of studies on the structure and function in diverse media (Vogel & Jähnig, 1986).

In water melittin can undergo a monomer–tetramer aggregation (Faucon et al., 1979; Talbot et al., 1979; Lauterwein et al., 1980; Brown et al., 1980; Bello et al., 1982; Quay & Condie, 1983). At acidic or neutral pH and concentrations $\lesssim$1 mM the peptide assumes a largely random-coil monomeric conformation. Adding salt and/or raising the pH results in the formation of tetramers with pronounced secondary structure. There is no indication that appreciable amounts of dimers or trimers occur (Schubert et al., 1985). The degree of self-association as a function of the total peptide concentration could be quantitatively described in terms of a simple mass action law for the reaction $4M_1 \rightleftharpoons M_4$ (M_1 and M_4 being the monomeric and tetrameric species). This has been shown on the basis of measuring the inherent shift of the wavelength of maximum fluorescence emitted by the Trp-19 residue (Quay & Condie, 1983).

In the present paper we report on kinetic data of the tetramerization process, as they are obtained by means of a stopped-flow instrument. In contrast to a recent approach where circular dichroism was used (Salerno et al., 1984), a fluorescence signal has been followed here. This permitted a better time resolution. An analysis of our experimental results leads to a simple rate law which suggests a straightforward reaction mechanism involving slow dimerization followed by a fast assembly of two dimers.

Materials and Methods

Melittin, grade II, phospholipase free, was purchased from Sigma Chemical Co. (St. Louis, MO). This product has been shown to contain about 20% peptide which is formylated at the amino terminal (Lauterwein et al., 1980). By means of electrophoresis and HPLC runs we have found that our sample is indeed composed of two different species at a ratio of approximately 4 to 1. These are presumed to be the unformylated and formylated melittin modifications, respectively. Both are, however, equivalent under the conditions of our experiments (see Discussion). Hence, the commercial sample was used without further purification in order not to waste material needlessly. All other reagents were of the highest purity commercially available (Merck AG, Darmstadt, West Germany).

The peptide concentration was determined from ultraviolet absorption, recorded on a Varian Techtron 634, by applying a molar optical absorption coefficient $\epsilon = 5570\ M^{-1}\ cm^{-1}$ at 280 nm (Quay & Condie, 1983).

Uncorrected fluorescence spectra were registered with a Schoeffel RRS 1000 fluorometer (excitation at 280 nm with 2-nm bandwidth, emission in the range of 300–400 nm with 3.5-nm bandwidth). For the evaluation of λ_0, i.e., the peak emission wavelength, we adopted the method of averaging the wavelengths at half-maximum fluorescence (Quay & Condie, 1983).

The kinetic experiments were carried out in a thermostated Durrum stopped-flow apparatus (dead time 2.8 ms) equipped with two monochromators and a fluorescence detection system as developed in this department (Paul et al., 1980), the fluorescence being excited at 282 nm (7-nm bandwidth). Aggregation or dissociation was monitored by the fluorescence intensity F, emitted above 345 nm (with a WG 345 cutoff filter in front of the photomultiplier). In order to correct for lamp instabilities and to improve the resolution of measurement, we actually recorded relative deviations from an appropriate reference. A certain part ($\approx$10%) of the original lamp light intensity was split off and converted electrically to a fixed signal F_R of about the magnitude of F_∞, the fluorescence signal eventually observed at equilibrium after mixing. The relative signal then registered is

$$\phi = (F - \alpha F_R)/F_R \qquad (1)$$

involving a somewhat adjustable factor α ($\approx$1) which permits fine tuning of the definite reference. We have set α so that $\alpha F_R = F_\infty$, implying $\phi \rightarrow 0$ in the given experiment. The complete time course of ϕ was picked up by a DL 905 transient

† This work was supported by Grant 3.285.85 from the Swiss National Science Foundation.

0006-2960/88/0427-7826$01.50/0

recorder and was then stored permanently on a disk.

In all our experiments we maintained a temperature of 23.5 °C and a pH of 8.1 (10 mM Tris-HCl). In order to avoid the inner-filter effect in the fluorescence measurements, the melittin concentration was kept below an upper limit of about 400 μM. The need for a sufficient signal to noise ratio, on the other hand, implied a lower limit around 1 μM in the equilibrium and 10 μM in the kinetic experiments. The solutions used for the stopped-flow work have always been carefully degased.

Results

Equilibrium Properties. According to the mass action law for a monomer–tetramer self-association, an appropriate aggregation constant is defined as $K_a = \bar{c}_4/\bar{c}_1^4$ (c_1 and c_4 being the concentrations of the monomeric and tetrameric species, respectively, with a bar indicating equilibrium conditions). We introduce a degree of aggregation $x = 4c_4/c_P$, where c_P stands for the total concentration of peptide ($=c_1 + 4c_4$). Then the mass action law implies that

$$\bar{x}/(1 - \bar{x})^4 = 4K_a c_P^3 = 8(c_P/c_P^*)^3 \qquad (2a)$$

involving a "critical concentration"

$$c_P^* = (2/K_a)^{1/3} \qquad (2b)$$

At this concentration of melittin, just half of the total amount of peptide exists in the aggregated state ($\bar{x} = 1/2$).

Adding an electrolyte promotes the aggregation, presumably due to electrostatic screening of the positive charges on the peptide chains. This effect can be practically utilized to induce or suppress the self-association process. However, rather high concentrations of a simple univalent electrolyte such as NaCl are required to attain a c_P^* in our experimental range of melittin concentrations. A salt with divalent anions such as Na_2SO_4 is much more effective (Tatham et al., 1983). Therefore we have chosen the latter electrolyte to control the extent of aggregation.

The magnitudes of K_a and c_P^* for a given molarity of the sodium sulfate, [Na_2SO_4], have been determined by means of measuring λ_0 at various c_P. The evaluation procedure is based on the relation

$$\lambda_0 = \lambda_{01}(1 - \bar{x}) + \lambda_{04}\bar{x}$$

with λ_{01} and λ_{04} being the λ_0 values of the purely monomeric and tetrameric forms. This has been established to be a good approximation under the given circumstances (Quay & Condie, 1983). By inspection of our data at the limit of small c_P (where $\bar{x} \approx 0$), we obtain $\lambda_{01} = 354.1$ (±0.1) nm in good agreement with the previously reported 353.7 (±0.2) nm. The λ_{04} is extrapolated at large c_P where eq 2 leads to the relation $\bar{x} \approx 1 - (c_P^*/2c_P)^{3/4}$. Then one may write

$$\lambda_0 = \lambda_{04} + (\lambda_{01} - \lambda_{04})(c_P^*/2)^{3/4} c_P^{-3/4}$$

Accordingly, a plot of λ_0 versus $c_P^{-3/4}$ permits a linear extrapolation yielding λ_{04} as the intercept on the λ_0 axis. This approach was successfully applied to three aqueous melittin systems with [Na_2SO_4] = 0.18, 0.108, and 0.054 M, respectively. In any of these cases we arrived at linear plots involving the same intercept of $\lambda_{04} = 342.5$ (±0.1) nm, perfectly in line with the value of Quay and Condie (1983).

Having evaluated $\bar{x}$ from λ_0, we plotted log [$\bar{x}/(1 - \bar{x})^4$] versus log c_P. Because of eq 2a, a straight line with a slope of 3 should fit the data. This is indeed so as shown for the examples in Figure 1. The K_a and c_P^* obtained for a number of salt concentrations are compiled in Table I. These values have been used to calculate the pertinent self-association curves presented in Figure 2.

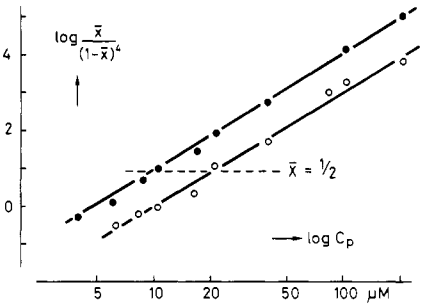

FIGURE 1: Double logarithmic plots of $\bar{x}$, the degree of self-association at equilibrium, according to eq 2a (c_P: melittin concentration) for two concentrations of added sodium sulfate, 0.108 (●) and 0.054 M (○). The straight lines have a slope of 3 corresponding to a tetramerization process.

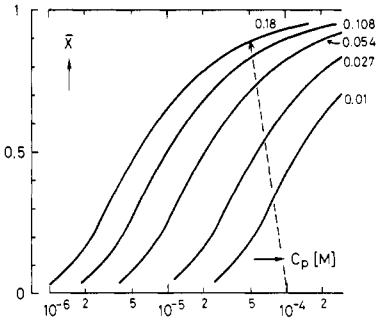

FIGURE 2: Equilibrium degree of tetramerization, $\bar{x}$, plotted versus the total peptide concentration for various fixed concentrations of added Na_2SO_4 (indicated in molarity). The appropriate K_a are those of Table I. No added salt implies $\bar{x} = 0$ in the given range of c_P. These curves have been used in the kinetic experiments for a determination of the initial and final values of x, denoted x_0 and x_∞, respectively (see text). The dashed arrow, for instance, corresponds to a jump of $\bar{x}$ in a mixing experiment where a salt-free melittin solution of 10^{-4} M is diluted by a 0.36 M Na_2SO_4 solvent, resulting in a final concentration of 5 × 10^{-5} M in 0.18 M salt ($x_0 = 0 \rightarrow x_\infty = 0.89$).

Table I: Aggregation Constants, K_a, Critical Concentrations, c_P^*, and Rate Constants, k_a and k_{-a} (for the Association and Dissociation Reactions, Respectively), of the Melittin Tetramerization in Aqueous Solution (23.5 °C, pH 8.1) at Various Concentrations of Added Sodium Sulfate[a]

[Na_2SO_4] (M)	K_a (M^{-3})	c_P^* (μM)	k_a (10^5 M^{-1} s^{-1})	k_{-a} (10^{-3} $M^{1/2}$ s^{-1})
0.0	$\lesssim 3 \times 10^8$	$\gtrsim 2 \times 10^3$		
0.01	9.1×10^{11}	130		
0.027	1.1×10^{13}	56.7	1.0	30
0.054	2.3×10^{14}	20.6	1.4	9.2
0.108	2.2×10^{15}	9.7	2.2	4.7
0.18	1.1×10^{16}	5.65	3.8	3.6

[a] We note that a plot of log k_a versus the square root of [Na_2SO_4] can be fitted by a straight line (with a linear correlation coefficient r = 0.9990).

Basic Stopped-Flow Experiment. We always started with two solutions, denoted I and II. The first one contained melittin at a concentration of $2c_P$ and a salt concentration $[Na_2SO_4]_I$ and the second no melittin and a salt concentration $[Na_2SO_4]_{II}$. Equal volumes of I and II have been mixed rapidly so that the peptide concentration is reduced to c_P. The initial degree of self-association x_0 is determined by $[Na_2SO_4]_I$ and can be read from the appropriate curve in Figure 2 at the position $2c_P$. Since the dilution and also the possible change of electrolyte concentration generally perturb the aggregation equilibrium, the degree of aggregation will adjust itself to the new conditions in the course of time. The final equilibrium

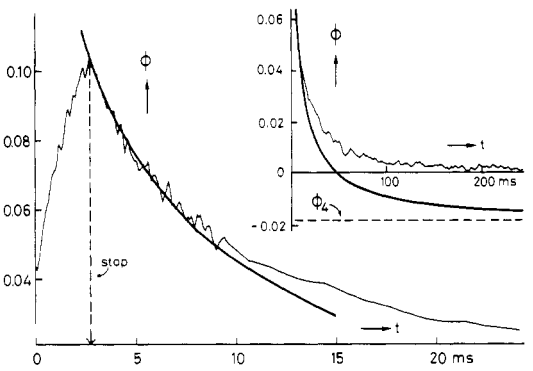

FIGURE 3: Specimen record of the fluorescence signal ϕ ($\phi \rightarrow 0$ for $t \rightarrow \infty$; α is 0.865) versus time after having mixed 4×10^{-4} M melittin (no salt) with 0.216 M Na_2SO_4 so that $c_P = 2 \times 10^{-4}$ M at 0.108 M salt (then x changes from $x_0 = 0$ to $x_\infty = 0.90$). As for stop and zero time, see text. The smooth curve represents the pure association reaction which is to fit the initial part of the measured record. It has been calculated according to eq 6a with b, ϕ_4, and k as specified in Figure 4. The inset shows the same record as well as the fitting curve in the later phase of the reaction. These must necessarily diverge in the long run because of the growing effect of the reverse reaction, i.e., dissociation, which has been neglected in the present fitting approach. The final deviation is in fact equal to the value of $-\phi_4$ computed with $x_\infty < 1$ as determined in the equilibrium experiments.

value x_∞ is the one taken in Figure 2 at a concentration c_P for the average salt concentration of I and II (for example, the arrow in Figure 2 refers to an experiment where a salt-free 10^{-4} M melittin solution is mixed with a 0.36 M Na_2SO_4 solution).

As was mentioned above, we follow the time course of the reaction by means of the fluorescence emission at $\lambda \gtrsim 345$ nm (see Materials and Methods): $F = F_1(1 - x) + F_4x$. The appropriate quantities F_1 and F_4 for the purely monomeric and tetrameric states have been determined with a salt-free solution (where $x = 0$) to which sufficient salt has been eventually added (so that $x \rightarrow 1$). This resulted in $F_4/F_1 = 0.82$ (± 0.02). In other words, upon tetramerization the measurable fluorescence emission undergoes a relative drop of $f_{14} = (F_1 - F_4)/F_1 = 0.18$ (± 0.02). Hence, $F = (1 - f_{14}x)F_1$, and the actual measuring signal being recorded (see eq 1) becomes

$$\phi = b(x_\infty - x) \tag{3a}$$

where

$$b = \alpha f_{14}/(1 - f_{14}x_\infty) = \phi_1 - \phi_4 \tag{3b}$$

The signals

$$\phi_1 = bx_\infty \tag{3c}$$

and

$$\phi_4 = -b(1 - x_\infty) \tag{3d}$$

correspond to purely monomeric and tetrameric peptide states, respectively. Vice versa, we have

$$1 - x = (\phi - \phi_4)/b \tag{4}$$

Accordingly, the experimental ϕ curves can be directly related to the time dependence of the degree of aggregation.

Association Kinetics Approach. In a first series of experiments, we have chosen conditions which permit the dissociation reaction (i.e., $M_4 \rightarrow 4M_1$) to be practically neglected during a longer initial phase so that the kinetics is essentially controlled by the association reaction $4M_1 \rightarrow M_4$. This is expected to apply when a salt-free melittin solution (where $x_0 = 0$) is mixed with a sufficiently concentrated salt solution ($[Na_2SO_4]_{II} > 0.05$ M so that $x_\infty \gtrsim 0.9$), as done for instance in the experiment of Figure 3. Under such circumstances a most extensive change of x is induced, yielding a fairly good level of signal.

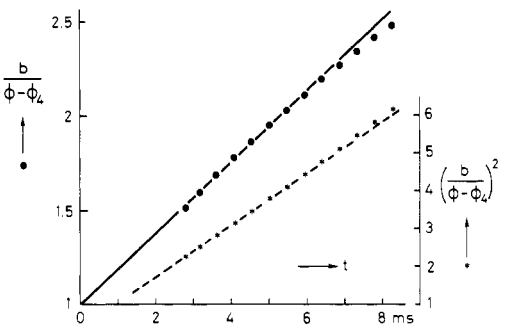

FIGURE 4: Analysis of the kinetic curve of Figure 3 (where $b = 0.1858$ and $\phi_4 = -0.0186$). A plot of $b/(\phi - \phi_4)$ versus time (●) can be fitted by a straight line through unity on the ordinate axis (the slope is $k = 185$ s^{-1}). This complies with a second-order rate of association (see eq 6a). The bending of the data points at longer times is attributed to the slowing down caused by the reverse reaction. A third-order kinetics can definitely be ruled out in view of the alternative plot of the square of $b/(\phi - \phi_4)$ versus time (*). With $m = 3$ in eq 5, it follows that this plot must linearly extrapolate to unity at $t = 0$, which is clearly not true here. In addition, the eventual bending of the data points turns to the wrong direction (indicating a physically unreasonable speeding up of the total rate).

Let us assume a simple rate law of an integral order m for the association, i.e.

$$(dc_4/dt)_a = k_a c_1^m \rightarrow dx/dt = 4k_a c_P^{m-1}(1 - x)^m$$

with k_a being the pertinent rate constant. By integration one arrives at

$$[(1 - x_0)/(1 - x)]^{m-1} = 1 + 4(m - 1)k_a c_P^{m-1}t \tag{5}$$

It turned out that our measured kinetic curves could be well fitted in a consistent way only for $m = 2$, indicating a second-order kinetics of the association reaction. In consideration of eq 4 we then obtain

$$1/(1 - x) = b/(\phi - \phi_4) = 1 + kt \tag{6a}$$

with a characteristic time constant

$$k = 4k_a c_P \tag{6b}$$

In a given experiment (see the example of the Figures 3 and 4) the quantities b and ϕ_4 are determined from known values of α, f_{14}, and x_∞ by application of eq 3b, 3c, and 3d. The fast part of the recorded ϕ curve can now be fitted by the function of eq 6a once the k is properly adjusted (note that due to the neglect of the reverse reaction there is naturally no fit at longer times; see figure 3). In the present approach an apparent start of the reaction ($t = 0$) at 2.8 ms before the stop time has been considered, the latter being marked by the peak of the registered signal (see Figure 3). The so-defined zero time was extrapolated independently on the basis of a suitable method (Paul et al., 1980).

We tried to fit the kinetic curves analogously with $m = 1$ and 3, respectively. These attempts clearly failed (see Figure 4).

On the basis of sets of b, ϕ_4 evaluated for various concentrations of melittin and sodium sulfate, the respective characteristic time constants were determined by the described fitting procedure. The results are presented in Figure 5. At a fixed $[Na_2SO_4]$ we find in fact that k increases proportionally to c_P in accordance with eq 6b. The individual second-order rate constants k_a (see Table I) are seen to increase upon raising the salt concentration.

Relaxation Kinetics Approach. Within our accessible range of melittin concentrations the above association kinetics ap-

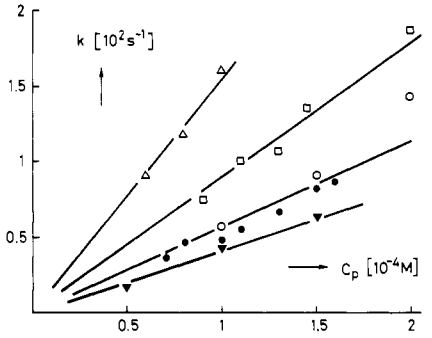

FIGURE 5: Plots of the time constant, k, versus the peptide concentration, c_P, for various Na_2SO_4 concentrations (M): 0.18 (△); 0.108 (□); 0.054 (○, ●); 0.027 (▼). This includes results of the association kinetics approach (open points) and of the relaxation kinetics approach (full points).

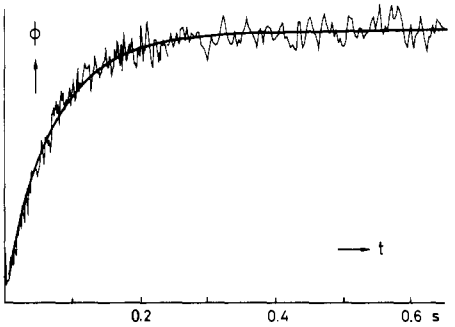

FIGURE 6: Record of the fluorescence signal ϕ (arbitrary units) for a dilution experiment where the relaxation kinetics approach can be applied. A 2×10^{-4} M peptide solution in aqueous 0.054 M Na_2SO_4 is mixed with the peptide-free solvent (so that $x_0 = 0.89 \rightarrow x_\infty = 0.82$ at $c_P = 10^{-4}$ M in 0.054 M salt). The smooth curve is an exponential fit involving a relaxation time $\tau_0 = 70$ ms.

proach requires jumps of the salt concentration from very low to quite high. Nevertheless the basic stopped-flow experiment can as well be performed under more general salt conditions. This will, however, usually involve comparatively small changes of the degree of aggregation. Then only a rather low level of the measuring signal is encountered. In addition, we must consider the dissociation rate even in the initial course of the reaction.

We have carried out a series of such experiments with smaller $|x_0 - x_\infty|$, especially at lower salt concentrations. In order to improve the signal to noise ratio, records of 20–30 equivalent experiments have been averaged. It was found that the kinetic curves can be well fitted by an exponential time function (see Figure 6). The respective relaxation times τ_0 are essentially determined by the initial slope of the signal. Such "initial relaxation times" are related to the forward and reverse rate laws in any case of a perturbation of equilibrium (Schwarz, 1968, 1986).

Naturally the dissociation rate must be consistent with a second-order forward rate and the given mass action law. Most simply, we may set

$$(dc_4/dt)_{-a} = k_{-a}c_4^{1/2} \tag{7a}$$

$$k_a/k_{-a} = K_a^{1/2} \tag{7b}$$

The overall rate equation for x can then be written

$$dx/dt = k\varphi(x, x_\infty) \tag{8a}$$

$$\varphi(x, x_\infty) = (1 - x)^2 - (1 - x_\infty)^2(x/x_\infty)^{1/2} \tag{8b}$$

This cannot easily be integrated in a rigorous way. A practically sufficient approximation resulting in an exponential course of x at a conserved initial slope is obtained by a linear interpolation of $\varphi(x, x_\infty)$ between x_0 and x_∞. So it follows that

$$1/\tau_0 = k\varphi(x_0, x_\infty)/(x_\infty - x_0) \tag{9}$$

which permits k to be determined from experimental values of τ_0 and the x_0 and x_∞ calculated on the basis of equilibrium data. We have utilized this relaxation kinetics approach in a number of experiments at salt concentrations of 0.054 and 0.027 M. The resulting k have been entered in Figure 4. In particular, we emphasize that these k are in line with the results of the association kinetics approach for the 0.054 M Na_2SO_4 case where both approaches could be applied.

Discussion

The question may be raised whether our results are possibly blurred because of the impurity of our commercial material containing some formylated melittin. The latter species has been indicated to aggregate appreciably better than the unformylated peptide form at lower pH. This effect is apparently caused by the inherent lack of a positive charge on the N-terminus (Lauterwein et al., 1980). The same feature largely applies, however, also to the unformylated amino end at our special pH of 8.1. That group will be almost fully deprotonated there, as follows from the reported pK values of 6.8 in the monomeric state (Bello et al., 1982) and of 6.95 in the tetrameric one (Stanislawski & Rüterjans, 1987). Hence, we may expect that in the present case practically all our melittin molecules are uncharged at the Gly-1 position and accordingly are equivalent as far as the tetramerization process is concerned. In fact, we could not observe significant differences between the results of test experiments with purified unformylated melittin, prepared according to the procedure of Batenburg et al. (1987), and the results obtained when the unpurified commercial sample was used.

The established second-order kinetics of the association suggests a slow dimerization to be the rate-determining step in the overall aggregation process. The final dimer–tetramer conversion must be comparatively fast. Then the question arises how this actually is accomplished. Apparently, either one of two basic pathways may be followed, involving (i) a dimer–dimer assembly or (ii) a dimer which successively combines with two monomers via a transient trimer state. It turns out that the first one can in fact be brought well into line with our experimental data whereas the second alternative must be ruled out because it leads to contradictions (see Appendix).

Therefore, we propose a straightforward mechanism of tetramerization described by two steps, namely

dimerization

$$2M_1 \underset{k_{-1}}{\overset{k_1}{\rightleftharpoons}} M_2 \qquad \text{(slow)} \tag{10a}$$

dimer–dimer assembly

$$2M_2 \underset{k_{-2}}{\overset{k_2}{\rightleftharpoons}} M_4 \qquad \text{(fast)} \tag{10b}$$

The dimer M_2 is assumed to occur as a steady-state intermediate of low concentration so that always

$$\xi = 2c_2/c_P \ll 1 \tag{10c}$$

On the other hand, in order to make the second step sufficiently fast, the condition

$$2k_2c_2 \gg k_{-1} \tag{10d}$$

must apply. This requires a rate constant k_2 close to the diffusion-controlled limit.

For the sake of simplicity we disregard the existence of a slow exchange reaction between two monomeric forms in the absence of added salt (Lauterwein et al., 1980). The low-abundant one of these forms has been estimated to constitute less than 10% of the total peptide. Within our inacccuracy of measuring we did not see any effect which could possibly be attributed to that second monomer state.

On the basis of the proposed scheme of reactions with its inherent steady-state condition for M_2 [i.e., $dc_2/dt \approx 0$ or $dc_4/dt \approx -(1/4)dc_1/dt$, respectively], the rate of tetramerization generally becomes

$$dc_4/dt = k_2c_2^2 - k_{-2}c_4 \approx (1/2)(k_1c_1^2 - k_{-1}c_2) \quad (11)$$

In the range of our association kinetics approach $k_{-2}c_4$ may be neglected. Because of eq 10d we then arrive at a second-order rate law:

$$dc_4/dt \approx k_a c_1^2 \quad (12)$$

where $k_a = k_1/2$. (If eq 10d did not apply, an apparent reaction order definitely larger than 2 would evolve.) Let us turn now to the situation of our relaxation kinetics approach. We note that upon an induced perturbation of the overall equilibrium a comparatively fast reequilibration of step 10b will take place because of condition 10d. Hence the relation $k_2c_2^2 \approx k_{-2}c_4$ is adjusted almost instantaneously. The c_2 in the slow dimerization term of eq 11 may be expressed with regard to c_4 resulting in an overall rate

$$dc_4/dt \approx k_a c_1^2 - k_{-a}\sqrt{c_4} \quad (13a)$$

where

$$k_{-a} = (k_{-1}/2)/\sqrt{K_2} \qquad (K_2 = k_2/k_{-2}) \quad (13b)$$

Evidently these features of the proposed mechanism are fully consistent with the phenomenological rate laws reflected by our experimental data as pointed out above. This does not apply for the simple alternative pathway of dimer–tetramer conversion through $M_2 + 2M_1 \rightleftharpoons M_4$, as demonstrated in the Appendix.

However, the present mechanism calls for a rather large rate constant k_2. It may be estimated with the relation

$$k_{-1} = 4k_a(1 - x_\infty)^2 c_P/\xi_\infty$$

which is derived from the rate balance of step 10a at final equilibrium. The crucial condition 10d accordingly implies that

$$k_2 \gg 4k_a(1 - x_\infty)^2/\xi\xi_\infty$$

where dimer contents ξ (in the transient steady state) and ξ_∞ (at final equilibrium) up to a few percent may be possible. In view of the k_a and x_∞ in our experiments, a minimum order of magnitude of 10^8 M^{-1} s^{-1} for k_2 is indicated. On the other hand, k_2 cannot be larger than its upper limit of about 3×10^9 M^{-1} s^{-1} owing to diffusion control (see Appendix). Therefore, dimer contents much below 1% have to be excluded.

We note that the overall monomer–tetramer turnover includes a conformational transition of the monomeric chains. Presumably this structural change occurs in the dimerization step. Then the slow dimerization rate could be attributed to a rate-limiting change of secondary structure. The rate constant would be in the range of 10^4–10^5 s^{-1} as pointed out in more detail in the Appendix. Such an order of magnitude appears quite reasonable physically. Hardly realistic values $\gtrsim 10^8$ s^{-1} would, however, be indicated for a conformational change in the fast dimer–dimer assembly. Along these lines the proposed mechanism may be rationalized with respect to the tetramer structure determined by Terwilliger et al. (1982). This structure is actually composed of two identical dimers. Each comprises two largely helical peptide chains with some hydrophobic interaction which may ensure some stability of a single dimer. Let us assume that these dimers are formed from ordinary unordered monomers in a comparatively slow reaction. Two of them can then readily associate toward the final tetramer practically as fast as diffusion control permits. The observed enhancement of k_a upon increasing the salt concentration is attributed to the electrostatic screening effect exerted on the positive charges carried by the peptide chains.

More direct kinetic studies of the conformational changes accompanying melittin aggregation have recently been done by monitoring circular dichroism (Salerno et al., 1984). The experimental procedure was the same as adopted in our association kinetics approach. The so-measured kinetic curves exhibit two phases of the reaction, one falling in the dead-time period of the apparatus (≈5 ms) and another one in the 0.1–1-s range. The slow event should actually be visible in relaxation experiments irrespective of the nature of the measuring signal. However, our fluorescence curves, if recorded under comparable conditions of concentration, are faster by about a factor of 5. At present we have no explanation for this obvious difference of experimental results.

ACKNOWLEDGMENTS

We thank Drs. S. Stankowski and H. Vogel for helpful discussions. We also thank E. Kuchinka for her help in the characterization of our melittin sample and in the purification work.

APPENDIX

Another Pathway for Dimer–Tetramer Conversion. As a potential alternative for the fast dimer–dimer assembly in reaction scheme 10 we consider a pathway where a dimer associates rapidly with two monomers via two consecutive steps, namely

$$M_2 + M_1 \underset{k_{-3}}{\overset{k_3}{\rightleftharpoons}} M_3 \qquad M_3 + M_1 \underset{k_{-4}}{\overset{k_4}{\rightleftharpoons}} M_4$$

By applying the steady-state condition to the assumed low-population trimer state M_3, we may formally transform these steps to

$$M_2 + 2M_1 \underset{k'_{-2}}{\overset{k'_2}{\rightleftharpoons}} M_4$$

with the rate equation

$$dc_4/dt \approx k'_2c_1c_2 - k'_{-2}c_4$$

involving the apparent "rate constants"

$$k'_2 = [k_4c_1/(k_{-3} + k_4c_1)]k_3$$

$$k'_{-2} = [k_{-3}/(k_{-3} + k_4c_1)]k_{-4}$$

Owing to the steady-state condition for M_2, the rate of tetramerization then becomes

$$dc_4/dt \approx k'_2c_1c_2 - k'_{-2}c_4 \approx k_1c_1^2 - k_{-1}c_2$$

Accordingly, a second-order kinetics for the association process only emerges if

$$k'_2c_1 \gg k_{-1}$$

In other words, again the dimer–tetramer conversion (this time by $M_2 + 2M_1 \rightarrow M_4$) must be much faster than dimer dissociation.

In the relaxation kinetics approach analogous argumentation as for the former alternative leads to an overall rate

$$dc_4/dt = k_a c_1^2 - k_{-a}(c_4/c_1^2)$$

where $k_a = k_1$ and $k_{-a} = k_{-1}/K_3K_4(K_3 = k_3/k_{-3}; K_4 = k_4/k_{-4})$. The initial relaxation times, τ_0, calculated with this rate equation and the k_a values evaluated from the association kinetics data, always fall by about a factor of 4 below the τ_0 which have actually been measured. These differences are by far beyond the experimental uncertainties. Hence, we conclude that the present alternative pathway may be disregarded.

Effect of Diffusion Control. The reaction of two monomers to form a dimer M_2 may be formulated as

$$M_1 + M_1 \underset{k_{-d}}{\overset{k_d}{\rightleftharpoons}} (M_1M_1) \xrightarrow{k_i} M_2$$

involving the intermediate encounter complex (M_1M_1) which results from diffusional motions of the individual monomers (k_d and k_{-d} being the appropriate rate constants). The actual conversion to M_2 requires an internal transition of (M_1M_1) described by the pertinent rate constant k_i. The overall second-order rate constant for $M_1 + M_1 \rightarrow M_2$ so becomes

$$k_1 = [k_i/(k_i + k_{-d})]k_d \qquad \text{(A1)}$$

owing to the steady-state condition for (M_1M_1). The basic theory [see, e.g., Schwarz (1986)] leads to the expressions

$$k_d = 4\pi N_A D_1 d_0 \qquad k_{-d} = 6D_1/d_0^2$$

(N_A = Avogadro's number; D_1 = diffusion coefficient of M_1; d_0 = reaction distance, i.e., the distance between the M_1 in the encounter complex) provided the particles have spherical shape and do not electrostatically interact. The latter assumption practically applies also to charged particles if sufficient electrolyte is added to screen the interactions.

For the melittin monomers a spherical radius $R_1 \approx 9.5$ Å may be assumed (based on a molecular mass of 2840 g/mol and a specific volume of 0.75 cm^3/g). By application of Stokes law this leads to $D_1 \approx 2.5 \times 10^{-6}$ cm^2/s which agrees well with experimental values in the literature (Podo et al., 1982). With $d_0 = 2R_1$, we then arrive at

$$k_d \approx 3.5 \times 10^9 \text{ M}^{-1} \text{ s}^{-1} \qquad k_{-d} \approx 4 \times 10^8 \text{ s}^{-1}$$

These approximate values are seen to be only slightly affected due to possible deviations from the underlying assumptions regarding shape and interactions.

At any rate, the measured $k_1 = 2k_a$ are by orders of magnitude smaller than k_d. According to eq A1 the transition from the encounter complex to the dimer has a rate constant $k_i \approx 10^4$–10^5 s^{-1}. This appears to reflect an inherent rate-limiting change of secondary structure. We propose there is a specific conformation of the monomeric chains in the dimer. A practically instantaneous conversion to the final product may take place whenever proper conformations are assumed during the lifetime of an encounter complex (including possible cases where monomers have already undergone the structural transformation prior to the moment of encounter). With a sufficiently slow conformational transition most encounter complexes will then dissociate before a dimer can be formed. The overall rate accordingly becomes very much reduced.

Analogous reflections on the dimer–dimer assembly step yield the same k_d as above but a somewhat smaller k_{-d} of about 2×10^8 s^{-1}. Because of the required large k_2 as pointed out under Discussion, the transition (M_2M_2) $\rightarrow M_4$ must be associated with a rate constant $k_i \gtrsim 10^8$ s^{-1}.

References

Batenburg, A. M., Hibbeln, J. C. L., & de Kruijff, B. (1987) *Biochim. Biophys. Acta 903*, 155–165.

Bello, J., Bello, H. R., & Granados, E. (1982) *Biochemistry 21*, 461–465.

Brown, L. R., Lauterwein, J., & Wüthrich, K. (1980) *Biochim. Biophys. Acta 622*, 231–244.

Faucon, J. F., Dufourcq, J., & Lussan, C. (1979) *FEBS Lett. 102*, 187–190.

Habermann, E. (1972) *Science (Washington, D.C.) 177*, 314–322.

Knöppel, E., Eisenberg, D., & Wickner, W. (1979) *Biochemistry 18*, 4177–4181.

Lauterwein, J. L., Brown, R., & Wüthrich, K. (1980) *Biochim. Biophys. Acta 622*, 219–230.

Paul, C., Kirschner, K., & Hänisch, G. (1980) *Anal. Biochem. 101*, 442–448.

Podo, F., Strom, R., Crifo, C., & Zulauf, M. (1982) *Int. J. Pept. Protein Res. 19*, 514–527.

Quay, S. C., & Condie, C. C. (1983) *Biochemistry 22*, 695–700.

Salerno, C., Crifo, C., & Strom, R. (1984) *Eur. J. Biochem. 139*, 275–278.

Schubert, D., Pappert, G., & Boss, K. (1985) *Biophys. J. 48*, 327–329.

Schwarz, G. (1968) *Rev. Mod. Phys. 40*, 206–218.

Schwarz, G. (1986) in *Investigations of Rates and Mechanisms of Reactions* (Bernasconi, C. F., Ed.) Vol. 6, Part 2, pp 27–139, Wiley, New York.

Stanislawski, B., & Rüterjans, H. (1987) *Eur. Biophys. J. 15*, 1–12.

Talbot, J. C., Dufourcq, J., de Bony, J., Faucon, J. F., & Lussan, C. (1979) *FEBS Lett. 102*, 191–193.

Tatham, A. S., Hider, R. C., & Drake, A. F. (1983) *Biochem. J. 211*, 683–686.

Terwilliger, T. C., Weissman, L., & Eisenberg, D. (1982) *Biophys. J. 37*, 353–361.

Vogel, H., & Jähnig, F. (1986) *Biophys. J. 50*, 573–582.